Aust. J. Phys., 1995, **48**, 461–8

Helicon Wave Measurements in an Inductively Coupled Magnetoplasma*

Keiji Nakamura, Keiji Suzuki and Hideo Sugai

Department of Electrical Engineering, Faculty of Engineering,
Nagoya University, Furo-cho, Chikusa-ku, Nagoya 464-01, Japan.

Abstract

Small-amplitude test waves at 30–100 MHz are externally excited in an inductive rf plasma for a magnetic field of ~100 G, to obtain a full dispersion relation for helicon waves. Measured wavelengths agree well with theoretical ones, not only for the test waves but also for large-amplitude principal waves at the discharge frequency of 13·56 MHz. Absolute measurements of the radial magnetic field B_r of the large-amplitude helicon wave are carried out, and the r, θ and z components of the wave electric field are estimated to be $E_r \sim E_\theta \sim 8\,\mathrm{V\,cm^{-1}}$ and $E_z \sim 0{\cdot}7\,\mathrm{V\,cm^{-1}}$ at an rf power of 800 W.

1. Introduction

Recently, various types of low-pressure high-density plasmas have been developed as high efficiency sources for plasma processing. Among them, inductively coupled magnetoplasmas, the so-called helicon-wave excited plasmas, have attracted much attention since almost fully ionised plasmas can be easily achieved (Boswell *et al.* 1982; Boswell 1984; Zhu and Boswell 1989). The production of helicon plasmas and their application to materials processing and laser sources has been reviewed by Boswell (1993), Shoji *et al.* (1993) and others. The mechanism for high density plasma production is considered to be absorption of helicon wave energies via Landau damping, and the theoretical analysis and experimental results have been reported along these lines. For example, Chen (1991) has derived the dispersion relation of helicon waves in a uniform bounded plasma and also suggested that the high absorption efficiency of helicon waves is explained by Landau damping. On the other hand, Komori *et al.* (1991) have observed helicon waves at a discharge frequency in the plasma, and demonstrated that the helicon waves decay in line with the theory of Landau damping.

The Landau damping process requires a propagation distance, at least a few wavelengths, to transfer the wave energies to the electrons. However, high-density plasma columns shorter in length than one wavelength are readily produced in a regime of helicon discharges. In addition, a burst of beam electrons has been observed to be ejected from a discharge antenna region (Zhu and Boswell 1991), suggesting a new electron acceleration mechanism besides helicon waves, e.g. by

* Refereed paper based on a presentation to the Third Japan–Australia Workshop on Gaseous Electronics and Its Applications, held at Yeppoon, Queensland, in July 1994.

0004-9506/95/030461$05.00

antenna near fields. Therefore, more information is necessary on wave fields as well as near fields to understand the helicon source. Especially, the measurement of the z-component of the wave electric fields is very important because it is an essential factor governing the mechanism of rf power absorption in magnetised plasmas.

In the present paper, we examine helicon waves which propagate in an inductively coupled magnetoplasma. The dispersion relation for small-amplitude test waves is measured and compared with large-amplitude principal waves at a discharge frequency of 13·56 MHz. We also measure the absolute radial magnetic fields of helicon waves excited by a discharge antenna, and estimate the r, θ and z components of the wave electric fields.

2. Helicon Wave Fields and Dispersion for a Bounded Plasma

Helicon or whistler waves in a cold uniform cylindrical plasma of radius a bounded by a vacuum have been analysed by Klozenberg *et al.* (1965) using Maxwell's equations and modified Ohm's law:

$$\boldsymbol{E} = \boldsymbol{j} \,.\, \boldsymbol{B}_0/eN_0 + \eta \boldsymbol{j} + (\partial \boldsymbol{j}/\partial t)/\epsilon_0 \omega_{\mathrm{p}}^2 , \tag{1}$$

where $\boldsymbol{E}$ and $\boldsymbol{j}$ denote the electric field and current, η is the plasma resistivity, and $\boldsymbol{B}_0$ and N_0 are the stationary axial magnetic field and plasma density. Assuming a functional form for the wave fields of $Q(r)\exp[\mathrm{i}(m\theta + k_{\parallel} z - \omega t)]$, the characteristic equation for the axial wavenumber $k_{\parallel}$ of azimuthal mode m is obtained as

$$(\omega + \mathrm{i}\nu)(k_{\parallel}^2 + k_{\perp}^2) - \omega_{\mathrm{c}} k_{\parallel}(k_{\parallel}^2 + k_{\perp}^2)^{\frac{1}{2}} + \omega\omega_{\mathrm{p}}^2/c^2 = 0 , \tag{2}$$

where ν is the electron collision frequency, $k_{\perp}$ is the radial wavenumber, ω, ω_{c} and ω_{p} are the wave, electron cyclotron and electron plasma frequencies, and c is the speed of light. In the derivation of these equations, the plasma is assumed to be sufficiently dense ($\omega_{\mathrm{c}} \ll \omega_{\mathrm{p}}$).

The axial, radial and azimuthal magnetic fields of a wave are expressed in terms of first Bessel functions J_m of mth order:

$$\begin{aligned} B_z(r) &= A_1 J_m(k_{\perp 1} r) + A_2 J_m(k_{\perp 2} r) , \\ B_r(r) &= \mathrm{i} A_1 f_r(r) + \mathrm{i} A_2 g_r(r) , \\ B_\theta(r) &= A_1 f_\theta(r) + A_2 g_\theta(r) , \end{aligned} \tag{3}$$

where A_1 and A_2 are constants. Here $k_{\perp 1}$ and $k_{\perp 2}$ are the two roots of the radial wavenumber $k_{\perp}$ in equation (2): one corresponds to an electromagnetic helicon wave in a high density plasma and the other to an electrostatic space charge wave in a low density plasma (Trivelpiece and Gould 1959). The four radial functions which appear in the above equations are $f_r(r) = F(r, k_{\perp 1}, k_{\parallel}, k_1)$, $g_r(r) = F(r, k_{\perp 2}, k_{\parallel}, k_2)$, $f_\theta(r) = \mathrm{i}F(r, k_{\perp 1}, k_1, k_{\parallel})$ and $g_\theta(r) = \mathrm{i}F(r, k_{\perp 2}, k_2, k_{\parallel})$, where $k_j = (k_{\parallel}^2 + k_{\perp j})^{1/2}$ for $j = 1, 2$. The function $F(r, \alpha, \beta, \gamma)$ is defined as

$$F(r, \alpha, \beta, \gamma) = [m\gamma J_m(\alpha r)/r + \alpha\beta J_m'(\alpha r)]/\alpha^2 . \tag{4}$$

The boundary conditions at the plasma radius $r = a$ give the determinant equation

$$\begin{vmatrix} f_r(a) & g_r(a) & -k_{\parallel} a K_m(k_{\parallel} a) \\ f_\theta(a) & g_\theta(a) & m K_m(k_{\parallel} a) \\ J_m(k_{\perp 1} a) & J_m(k_{\perp 2} a) & k_{\parallel} a K_m(k_{\parallel} a) \end{vmatrix} = 0, \tag{5}$$

where K_m denotes the second kind of Bessel function of mth order. Equations (2) and (5) give the dispersion relation for helicon waves. The dispersion and collisional damping of helicon waves of symmetric mode ($m = 0$) in a cylindrical plasma has been reported to agree with this prediction (Sugai *et al.* 1978).

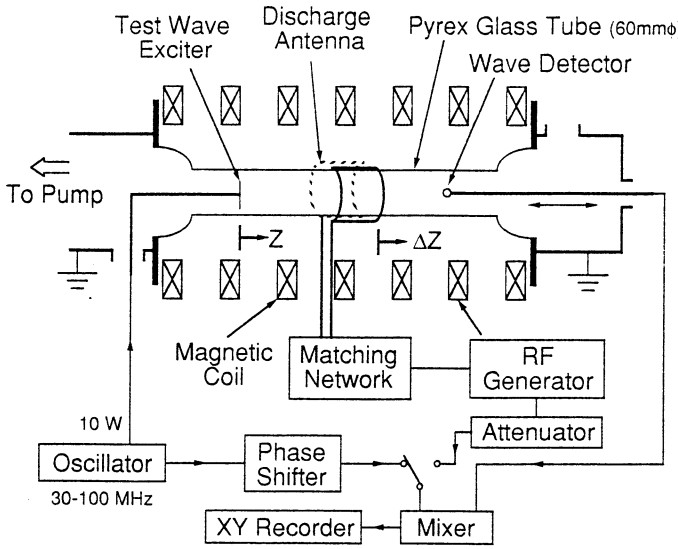

Fig. 1. Experimental apparatus.

3. Experimental

Fig. 1 is a schematic diagram of the experimental apparatus. A 1 m long and 6 cm diameter vacuum vessel made of pyrex glass is set along the centre axis of seven solenoid coils which give a dc magnetic field $\bar{B}$ along the z-axis from 60 to 130 G. Argon is fed through a mass flow controller at a typical operating pressure of 3 mTorr (1 mTorr $\equiv 0{\cdot}133$ Pa). A $13{\cdot}56$ MHz rf power of $\sim$800 W is inductively coupled with a discharge plasma through a Boswell type ($m = 1$) antenna of 11 cm in axial length, which is made of copper and located in the centre of the pyrex glass tube.

In order to obtain a full dispersion curve of helicon waves, small-amplitude test waves are externally excited by a 4 cm long dipole antenna located 17 cm away from the left edge of the discharge antenna. The dipole antenna induces radial electric fields and launches an asymmetric mode ($m = 1$) of waves at frequencies from 30 to 100 MHz with a small rf power of $\sim$10 W. The radial component

B_r of the wave magnetic field is detected by an 8 mm diameter one-turn loop antenna. The wave detector is rotatable in azimuth and movable axially along the z-axis over a range from the wave exciter of 2 to 47 cm (see Fig. 1). Using this detector, we can also measure the large-amplitude waves driven by the discharge antenna at 13·56 MHz with a large rf power of 800 W.

The wave propagation patterns are obtained by an interferometer method where a signal from the wave detector is mixed with a reference signal, and the mixer output, which is proportional to $B_r(z) \cos k_{\parallel} z$, is recorded as a function of the axial distance. When the wavelength is too long to determine by interferometry, the phase shift along z is directly measured by an oscilloscope. The absolute wave amplitudes are also obtained by calibrating the wave detector with known fields.

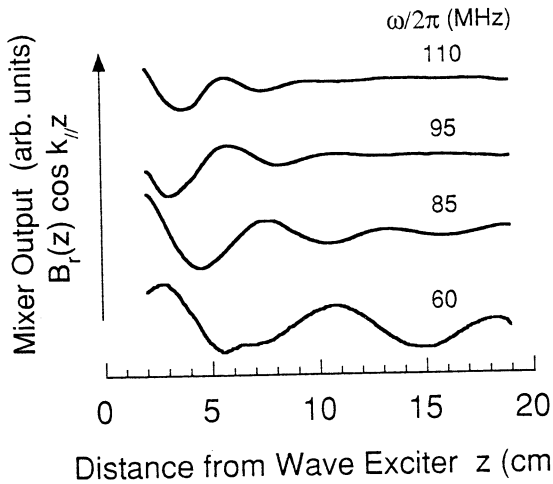

Fig. 2. Test wave propagation at different frequencies for $\bar{B} = 60$ G.

4. Results and Discussion

(4a) Small-amplitude Test Wave Propagation

Fig. 2 shows several examples of interferometer measurements of test wave propagation for a dc magnetic field of $\bar{B} = 60$ G ($\omega_c/2\pi = 168$ MHz), where the mixer output represents the axial variation of the amplitude $B_r(z)$ and the wave phase $\cos k_{\parallel} z$. As is well known, the helicon wavelength decreases with an increase in frequency, as clearly demonstrated in Fig. 2. A series of this kind of measurement gives the dispersion relation of the test wave, as shown in Fig. 3 where the normalised frequency ω/ω_c is plotted as a function of the axial wavenumber $k_{\parallel}$ multiplied by the collisionless plasma skin depth c/ω_p. The curve in Fig. 3 represents the theoretical dispersion of $m = 1$ helicon waves calculated from (2) and (5) for $\nu = 0$, where equation (4) has the singularities $J_1(k_{\perp} a) = 0$ and hence an approximate solution is given by $k_{\perp} a \sim 3{\cdot}83$ [the first root of $J_1(x) = 0$]. The electron number density of $4{\times}10^{11}$ cm^{-3} measured by a Langmuir probe was used in the calculation of ω_p. The measured dispersion

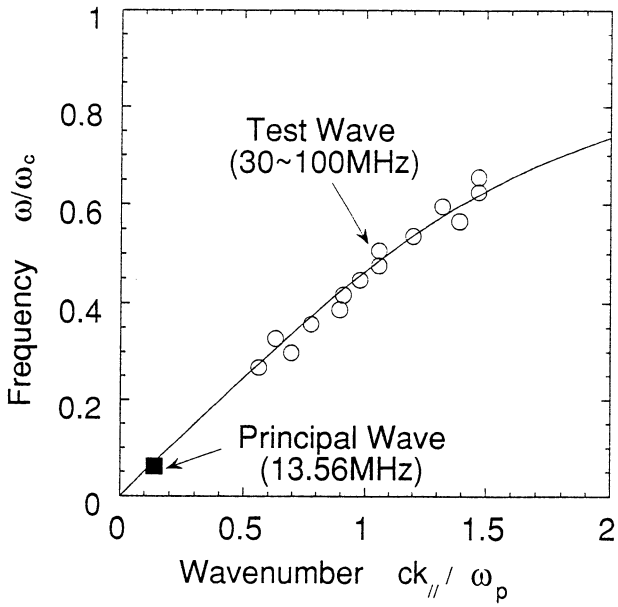

Fig. 3. Dispersion relation for test waves (circles) and principal wave (square), together with the theoretical prediction (curve) at $P_{\rm rf} = 800$ W.

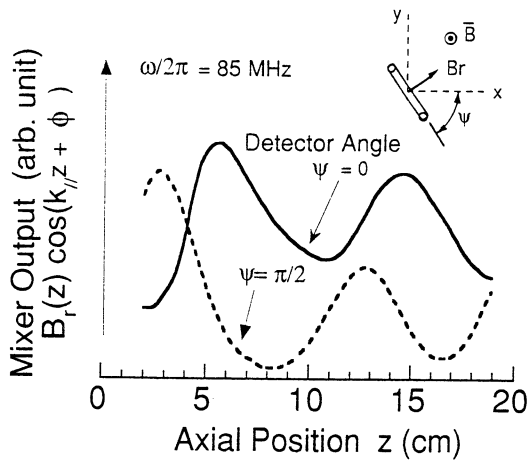

Fig. 4. Interferometer patterns for the wave detector angles $\psi = 0$ and $\pi/2$. The insert at top right illustrates azimuthal rotation of the wave detector.

relation agrees very well with the theoretical one, thus identifying the excited test waves to be helicon waves.

Furthermore, in order to examine polarisation of the test wave, the interferometer measurement was carried out by rotating the plane of the circular magnetic loop (wave detector) azimuthally by $\psi = \pi/2$ as shown in Fig. 4. The measured wave pattern axially shifts in phase by $\pi/2$, and hence the wave vector rotates in the

same direction as the electron cyclotron motion. As a consequence, the externally launched helicon wave is shown to be a right-hand circularly polarised wave.

(4b) Large-amplitude Principal Wave Propagation

Here we discuss the principal waves excited at 13·56 MHz by the discharge antenna, which have been thought to play a major role in plasma production. Fig. 5*a* shows the mixer output as a function of z, where the detector angle ψ defined in Fig. 4 is zero. As inferred from the theoretical dispersion curve shown in Fig. 3, the wavelength at 13·56 MHz and $\bar{B} = 60$ G ($\omega/\omega_c \approx 0{\cdot}08$) is very long (over 30 cm), making it difficult to obtain an accurate wavelength by the interferometer method. However, as shown in Fig. 5*b*, the phase shift $\Delta\phi$ measured by an oscilloscope is linearly proportional to the distance Δz from the edge of the discharge antenna (see Fig. 1). The slope of the line in the figure gives the precise wavelength $2\pi/k_{\parallel} \approx 42$ cm at $\bar{B} = 60$ G. These data for the 13·5 MHz wave are plotted as the square in Fig. 3, showing agreement

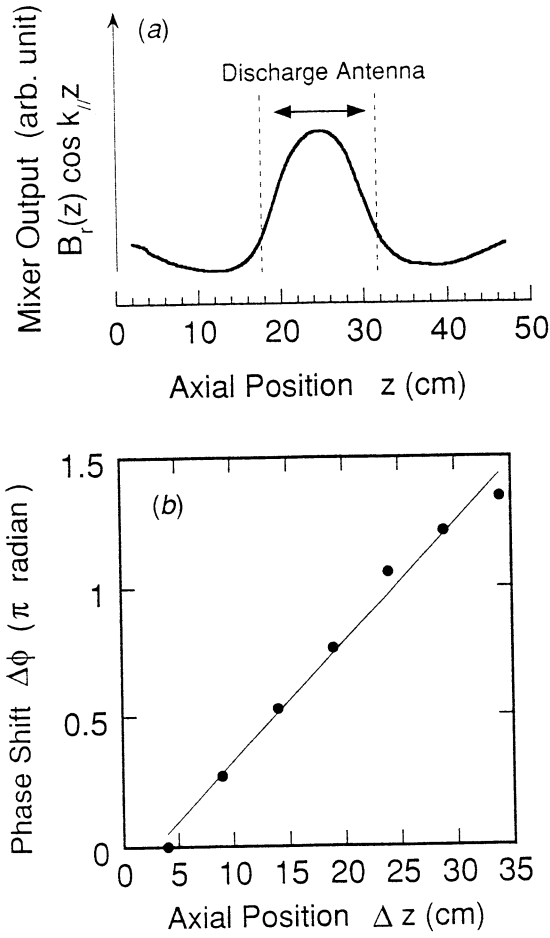

Fig. 5. Principal wave propagation at 13·566MHz showing the axial change of (*a*) the amplitude and phase measured by interferometry and (*b*) the phase measured by an oscilloscope, for $\bar{B} = 60$ G, $P_{rf} = 800$ W, 2 mTorr of argon and $\psi = 0$.

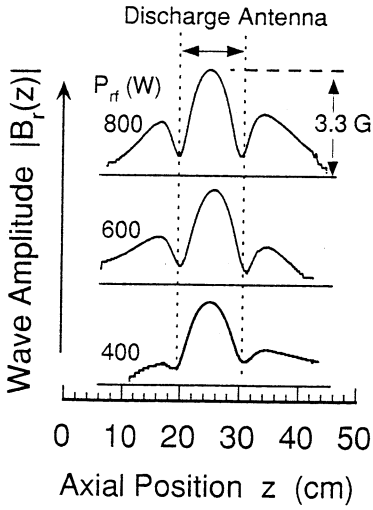

Fig. 6. Absolute qmplitude $|B_r|$ of the radial magnetic field of the principal wave (13·56 MHz) as a function of axial position for different rf powers, and for $\bar{B} = 60$ G, 3·6 mTorr of argon and $\psi = 0$.

with the theoretical dispersion. This result reveals that the 13·56 MHz helicon wave is actually launched from the discharge antenna.

Next, an absolute measurement of wave fields of 13·56 MHz was carried out as follows. The signal for the radial magnetic field $B_r(z)$ received by the wave detector is fed to both the reference and input ports of the mixer, and the mixer output is calibrated with the known magnetic fields. Fig. 6 shows the axial variation of the radial field B_r for different rf powers where $\psi = 0$. The amplitude B_r is strongest in the centre ($z \sim 25$ cm) of the antenna region for various rf powers, and falls to a minimum at both edges of the discharge antenna, suggesting the existence of standing waves in the plasma. The maximum value of B_r increases with the rf power to 3·3 G at 800 W. This value of B_r is comparable with the value reported by Shoji *et al.* (1993).

Furthermore, let us estimate the r, θ and z components of the electric field, E_r, E_θ and E_z, using the measured value of B_r. The axial electric field is given by the third term on the right-hand side of (1) as $E_z = -(\mathrm{i}\omega/\epsilon_0\omega_\mathrm{p}^2)j_z$, for $\eta = 0$ and axial current j_z. Substituting the magnetic fields given by (3) into Maxwell's equation

$$\nabla \times \boldsymbol{B} = \mu_0 \boldsymbol{j} \tag{6}$$

gives an axial current of order $|j_z| \sim |B_r|/\mu_0 a$. Thus, we find the amplitude ratio

$$|E_z/B_r| \sim (c^2/\omega_\mathrm{p}^2)(\omega/a)\,. \tag{7}$$

On the other hand, the transverse field $E_\perp$ for $\omega/\omega_\mathrm{c} \ll 1$ is mainly given by the first term in (1) as $|E_\perp| \sim (B_0/eN_0)|j_\perp|$, where (6) gives the transverse current $|j_\perp| \sim |B_z|/\mu_0 a$. Since $|B_z| \sim |B_r|$ from (3), we have the relation

$$|E_\perp/B_r| \sim (c^2/\omega_\mathrm{p}^2)(\omega_\mathrm{c}/a)\,. \tag{8}$$

From (7) and (8), the measured maximum value of $B_r = 36{\cdot}3$ G at 800 W gives $|E_z| = 0{\cdot}66\ \mathrm{V\,cm^{-1}}$ and $|E_r| \sim 8{\cdot}1\ \mathrm{V\,cm^{-1}}$.

5. Conclusion

We have experimentally investigated the dispersion characteristics and absolute wave fields of helicon waves in a 13·56 MHz inductively coupled magnetoplasma. A full dispersion relation for helicon waves in the plasma was obtained by exciting small-amplitude test waves externally at frequencies from 30 to 100 MHz. The measured dispersion relation agrees well with the theoretical prediction for a cylindrical plasma bounded by a vacuum in the case of test waves, as well as for large-amplitude principal waves at the discharge frequency. Absolute measurements of the radial magnetic field B_r of helicon waves were carried out, which allows an estimation of the electric fields of $E_z \sim 0{\cdot}7\,\mathrm{V\,cm^{-1}}$ and $E_r \sim E_\theta \sim 8\,\mathrm{V\,cm^{-1}}$ at the typical discharge power of 800 W.

Acknowledgments

The authors would like to thank Professor T. Watari for his courtesy in supplying the measuring instruments. This work was supported by a Grant-in-Aid for Scientific Research from the Ministry of Education, Science and Culture, in Japan.

References

Boswell, R. W. (1984). *Plasma Phys. Controlled Fusion* **26**, 1147.
Boswell, R. W. (1993). Proc. 21st Int. Conf. on Phenomena in Ionised Gases, Bochum (Eds G. Ecker *et al.*), p. 118 (Arbeitsgemeinschaft Plasmaphysik, Ruhr-Universität: Bochum).
Boswell, R. W., Porteous, R. K., Prytx, A., Bouchoule, A., and Ranson, P. (1982). *Phys. Lett.* A **91**, 163.
Chen, F. F. (1991). *Plasma Phys. Controlled Fusion* **33**, 339.
Klozenberg, J. P., McNamara, B., and Thonemann, P. C. (1965). J. Fluid Mech. **21**, 545.
Komori, A., Shoji, T., Miyamoto, K., Kawai, J., and Kawai, Y. (1991). *Phys. Fluids* B **3**, 893.
Shoji, T., Sakawa, Y., Nakazawa, S., Kadata, K., and Sato, T. (1993). *Plasma Sources Sci. Technol.* **2**, 5.
Sugai, H., Sato, M., Ido, K., and Takeda, S. (1978). *J. Phys. Soc. Jpn* **44**, 1953.
Trivelpiece, A. W., and Gould, R. W. (1959). *J. Appl. Phys.* **30**, 1784.
Zhu, P., and Boswell, R. W. (1989). *Phys. Rev. Lett.* **63**, 2805.
Zhu, P., and Boswell, R. W. (1991). *Phys. Fluids* B **3**, 869.

Manuscript received 6 October, accepted 18 November 1994